Energy scale of the electron-boson spectral function and superconductivity in $NpPd_5Al_2$

G. A. Ummarino
Dipartimento di Fisica, Politecnico di Torino, Corso Duca degli Abruzzi 24, 10129 Torino, Italy

R. Caciuffo
European Commission, Joint Research Centre, Institute for Transuranium Elements, Postfach 2340, D-76125 Karlsruhe, Germany

H. Chudo and S. Kambe
Advanced Science Research Center, Japan Atomic Energy Agency, Tokai-mura, Ibaraki 319-1195, Japan
(Received 7 June 2010; published 17 September 2010)

The energy scale Ω_0 of the electron-boson spectral function in the heavy-fermion, *d*-wave superconductor $NpPd_5Al_2$ is predicted on the basis of Eliashberg theory calculations. Assuming a spectral function shape typical for antiferromagnetic spin fluctuations, and imposing constraints provided by the experimental values for the critical temperature and the low-temperature energy gap, one obtains values of Ω_0 of about 2–2.5 meV, slightly dependent from the strength of the Coulomb pseudopotential. These values are in excellent agreement with the characteristic magnetic fluctuations energy estimated from NMR measurements of the nuclear-spin-lattice relaxation time at the Al site. The calculated temperature dependence of the upper critical field, the local spin susceptibility, and the nuclear-spin-lattice relaxation rate is also in good agreement with available experimental data, showing that a coherent description of the superconducting state can be obtained assuming that the electron pairing in $NpPd_5Al_2$ is mediated by antiferromagnetic fluctuations. We finally report predictions for the London penetration depth, the energy dependence of the tunneling differential conductance at different temperatures, and the temperature dependence of the energy gap.

DOI: 10.1103/PhysRevB.82.104510 PACS number(s): 74.20.Fg, 74.70.Tx, 74.20.Rp

I. INTRODUCTION

The properties of actinide compounds are often unusual. In systems with well-localized 5*f* electrons, in presence of unquenched orbital degrees of freedom and strong spin-orbit coupling, higher-order electromagnetic multipole interactions affect the ground state and the low-energy dynamics.[1] On the contrary, where the 5*f* states form narrow bands or are significantly hybridized with ligand- or conduction-electron states, the coexistence of atomic and metallic electron behavior can lead to distinct physics not described by the standard Landau-Fermi-liquid theory.[2]

Particularly interesting is the case of Pu- and Np-based heavy-fermion intermetallic superconductors, providing evidence for unconventional Cooper pairing not mediated by electron-phonon interactions.[3] A striking feature of these compounds is the value of the critical temperature, $T_c = 18.5$ K for $PuCoGa_5$ (Ref. 4) and 4.9 K for $NpPd_5Al_2$,[14] which is one order of magnitude higher than for typical *f*-electron superconductors. Several characteristics of the superconducting and normal states suggest that spin fluctuations may have an important role in the stabilization of the ground state of $PuCoGa_5$, although definite evidence on the nature of the mediating bosons is still missing.[6–8]

$NpPd_5Al_2$ is the only known superconducting Np compound. Following its discovery by Aoki *et al.*,[5] extensive studies on its physical properties have been reported.[9–12] $NpPd_5Al_2$ has a body-centered tetragonal crystallographic structure, with space group $I4/mmm$ and lattice parameters $a=4.1010$ Å and $c=14.6851$ Å at room temperature. The magnetic susceptibility in the normal phase follows the Curie-Weiss behavior and is strongly anisotropic. When the external magnetic field $\mathbf{B}$ is applied along the [100] direction, the effective paramagnetic moment μ_{eff} has a value of 3.2 μ_B/Np and the Curie-Weiss temperature is $\theta_p=-42$ K; for $\mathbf{B}\parallel[001]$, $\mu_{eff}=3.06$ μ_B/Np and $\theta_p=-139$ K. Electrical-resistivity and specific-heat measurements reveal a non-Fermi-liquid behavior of the normal phase, and the recovery of Fermi-liquid behavior in presence of magnetic fields larger than the upper critical field $H_{c2}(0)$.[12,13] With increasing pressure, the superconducting transition temperature T_c decreases and becomes zero above 5.7 GPa, indicating proximity to a quantum critical point.[13] The magnetic contribution to the electrical resistivity suggests the presence of Kondo interactions in a crystal-field potential, and the magnitude and overall temperature dependence of the thermoelectric power are typical of dense Kondo systems.[12] Mössbauer spectroscopy experiments indicates that the Np ions are nearly trivalent, and the negative sign of the Seebeck coefficient indicates that charge and heat transport are dominated by electrons,[12] in agreement with band-structure calculations.[14]

The temperature dependence of the electronic specific heat C_e suggests the presence of a large density of states at the Fermi level. In the temperature range between 1 and 3 K, the Sommerfeld coefficient $\gamma=C_e/T$ reaches a value of 325 mJ/mol K^2 when a magnetic field of 14 T is applied.[12] The specific-heat jump at T_c is $\Delta C_e/\gamma T_c=2.33$. Below T_c, C_e follows a T^2 dependence characteristic of strong coupling and suggesting the presence of line nodes in the energy gap $\Delta(T)$. The nuclear-spin-lattice relaxation rate $1/T_1$, deduced from ^{37}Al NMR spectra,[11] shows no coherence peak and varies, below T_c, as T^3. Assuming *d*-wave gap symmetry with line nodes, the observed temperature dependence gives[11] $2\Delta(0)/k_BT_c\simeq 6.4$. Above T_c, $1/T_1T$ decreases with increasing temperature, a behavior compatible with the presence of magnetic fluctuations.[11]

Electronic band-structure calculations[14] show the presence of a band with $5f$ character, having a large Fermi surface and a narrow bandwidth. This result supports the hypothesis that superconductivity in $NpPd_5Al_2$ involves $5f$ electrons. The possibility that nearly antiferromagnetic spin fluctuations provide the mediating bosons leading to d-wave pairing and superconductivity has been investigated by Tanaka and Hanzawa.[15] These authors calculate the dynamical susceptibility using a single-band Hubbard model with tight-binding dispersion and the fluctuation exchange approximation to study the effect of the on-site Coulomb repulsion.[15] Their results show that the features in the $NpPd_5Al_2$ band structure enhance strong incommensurate magnetic fluctuations favoring superconductivity with $d_{x^2-y^2}$ symmetry.[16]

Here, we report the results of d-wave Eliashberg theory[17–19] calculations performed in order to determine the energy scale of the mediating bosons spectral function that would be compatible with observed experimental data. We show that a spectral function centered around 2–2.5 meV is required to account for a critical temperature value $T_c \simeq 5$ K and an energy gap $\Delta(0)=1.35$ meV. These values compare very favorably with the characteristic magnetic fluctuations energy that can be deduced from ^{37}Al NMR measurements of the spin-lattice relaxation rate at the Al site.[20] The solutions of the Eliashberg equations are also used to calculate the temperature dependence of several physical observable, namely, the energy gap, the upper critical field, the London penetration depth, the local spin susceptibility, the nuclear-spin-lattice relaxation rate, and the energy dependence of the tunneling conductance. The good agreement between calculations and available experimental data indicates that the present model gives a coherent description of the superconducting state in $NpPd_5Al_2$ if the electron pairing is mediated by magnetic fluctuations.

II. THEORETICAL MODEL

In the imaginary-frequency-axis formulation, the d-wave one-band Eliashberg equations for the renormalization functions $Z(i\omega_n,\phi)$ and the gap $\Delta(i\omega_n,\phi)$ are given by[21]

$$\omega_n Z(i\omega_n,\phi) = \omega_n + \pi T \sum_m \int_0^{2\pi} \frac{d\phi'}{2\pi} \Lambda(i\omega_n - i\omega_m,\phi,\phi') \times N_Z(i\omega_m,\phi') + \Gamma_N \frac{N_Z(i\omega_n)}{c^2 + N_Z(i\omega_n)^2}, \quad (1)$$

$$Z(i\omega_n,\phi)\Delta(i\omega_n,\phi) = \pi T \sum_m \int_0^{2\pi} \frac{d\phi'}{2\pi} [\Lambda(i\omega_n - i\omega_m,\phi,\phi') - \mu^*(\phi,\phi',\omega_c)\vartheta(\omega_c - |\omega_m|)] N_\Delta(i\omega_m,\phi'), \quad (2)$$

where $\vartheta(\omega_c-|\omega_m|)$ is the Heaviside function, ω_c is an electronic cut-off energy for the Coulomb pseudopotential μ^*, $N_Z(i\omega_m,\phi)=\omega_m/\sqrt{\omega_m^2+\Delta^2(i\omega_m,\phi)}$, $N_Z(i\omega_n)$ is the average over ϕ of $N_Z(i\omega_n,\phi)$, $N_\Delta(i\omega_m,\phi)=\Delta(i\omega_m,\phi)/\sqrt{\omega_m^2+\Delta^2(i\omega_m,\phi)}$, and

$$\Lambda(i\omega_n - i\omega_m,\phi,\phi') = 2\int_0^{+\infty} d\Omega \frac{\Omega\alpha^2 F(\Omega,\phi,\phi')}{(\omega_n-\omega_m)^2+\Omega^2}. \quad (3)$$

Ω being the mediating boson frequency and $\alpha^2F(\Omega,\phi,\phi')$ the electron-boson spectral function.

The parameter Γ_N is proportional to the concentration of impurities or to disorder, and c is a parameter related to the electron phase shift for scattering off an impurity ($c=\infty$ with a constant value of Γ_N/c^2 corresponds to the Born limit, whereas the unitary limit is obtained when $c=0$).[22] The nth Matsubara frequency is defined as $i\omega_n = i\pi T(2n-1)$, with $n=0,\pm 1,\pm 2\ldots$, and T is the temperature.

In the following, calculations will be performed in the clean limit, that is assuming $\Gamma_N=0$, unless stated otherwise. As usual, we assume that $\alpha^2(\Omega)F(\Omega,\phi,\phi')$ and $\mu^*(\phi,\phi')$ contain at the lowest order separate s- and d-wave contributions, that is

$$\alpha^2F(\Omega,\phi,\phi') = \alpha^2F_s(\Omega) + \alpha^2F_d(\Omega)\sqrt{2}\cos(2\phi)\sqrt{2}\cos(2\phi'), \quad (4)$$

$$\mu^*(\phi,\phi') = \mu_s^* + \mu_d^*(\Omega)\sqrt{2}\cos(2\phi)\sqrt{2}\cos(2\phi'). \quad (5)$$

We adopt a simplified model, and we search for solutions of the Eliashberg equations with a pure d-wave symmetry gap function, $\Delta(\omega,\phi')=\Delta_d(\omega)\cos(2\phi')$, and a pure s-wave renormalization function, $Z(\omega,\phi')=Z_s(\omega)$. We note that, assuming d-wave symmetry for the gap function, the parameter μ_s^* does not enter into the two relevant Eliashberg equations. Therefore, although it is almost certainly large, it does not influence the solution. For simplicity, we finally assume that the normal density of states is constant around the Fermi level and that $\alpha^2F_s(\Omega)=\alpha^2F_d(\Omega)$.

The antiferromagnetic spin fluctuations spectral function for a uniform electron gas can be calculated in a T-matrix approximation,[23] and is proportional to a function $P(\Omega)=\Omega\Gamma/(\Omega^2+\Gamma^2)$, peaked at an energy Ω_0 of the order of Γ. For numerical calculation convenience, we approximate the corresponding Eliashberg spectral function as the difference of two Lorentzian curves, $\alpha^2F(\Omega)\propto[L(\Omega-\Omega_0,\Upsilon)-L(\Omega+\Omega_0,\Upsilon)]$, where $L(\Omega\pm\Omega_0,\Upsilon)=[(\Omega\pm\Omega_0)^2+(\Upsilon)^2]^{-1}$, Ω_0 is the energy of the peak, and Υ determines its half width at half maximum. We constrain the electronic cut-off energy to $\omega_c=24\Omega_0$ and the maximum quasiparticle energy to $\omega_{max}=32\Omega_0$.

III. CALCULATION OF THE MEDIATING BOSONS ENERGY SCALE

With the above assumptions, four free parameters remain, namely, λ_s, Ω_0, μ_d^*, and Υ. On the other hand, the experiments provide two constraints,[5,11] $T_c=5$ K and $\Delta(0)=1.35$ meV. We then proceed by assigning a value to μ_d^* and Υ, we calculate the $\lambda_s(\Omega_0)$ curve corresponding to a $T_c=5$ K by solving the Eliashberg equations, and for each value of Ω_0 we use the corresponding λ_s to calculate the

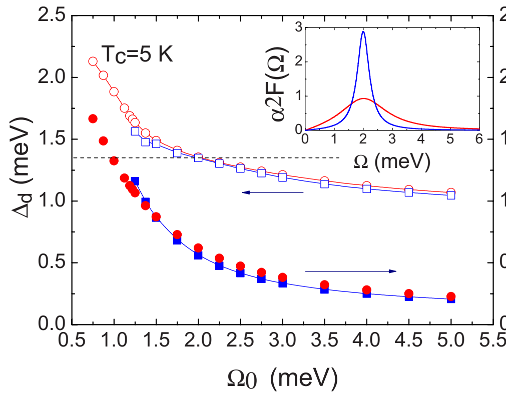

FIG. 1. (Color online) (Left axis) Gap values Δ_d calculated at T=0.25 K assuming a Coulomb pseudopotential μ_d^*=0, and an Eliashberg spectral function centered at an energy Ω_0 and having full width at half maximum Υ=1 meV (red, open circles) or Υ=0.25 meV (blue, open squares). The horizontal dashed line represents the experimental value of Δ_d. (Right axis) Electron-boson coupling constant λ_s as a function of Ω_0, for T_c=5 K, μ_d^*=0, and Υ=1 meV (red, closed circles) or Υ=0.25 meV (blue, closed squares). The inset shows the electron-boson spectral function in the two cases.

low-temperature gap, Δ_d, via Padè approximants.[24,25] The value of Ω_0 compatible with the experimental determination of Δ_d is then immediately determined. The calculations are repeated for different values of μ_d^* and Υ, to assess the influence of these parameters on the estimated energy scale of the electron-boson spectral function. The use of the Padè approximants technique for the calculation of Δ_d is preferable when dealing with strong-coupling superconductors because the value of $\Delta_d(i\omega_{n=0})$ obtained by solving the imaginary-axis Eliashberg equations can in these cases differ considerably from the value of Δ_d provided by the real-frequency-axis Eliashberg equations.[26]

Figure 1 shows the results of the procedure described above for μ_d^*=0, and Υ=1 meV or 0.25 meV. For Υ=1 meV, we obtain Ω_0=2 meV and λ_s=2.48; the value of Ω_0 does not change significantly if Υ is reduced to 0.25 meV, whereas λ_s decreases to 2.24. Indeed, the critical temperature T_c is an increasing function of both λ_s and of Ω_{log}, a characteristic energy of the electron-boson spectral function, $\Omega_{log}=\exp\{[2\int_0^{+\infty} d\Omega \ln(\Omega)\alpha^2F_s(\Omega)/\Omega]/\lambda_s\}$.[18] With decreasing Υ, Ω_{log} increases toward Ω_0 (Ω_{log}=1.29 meV for Υ=1 meV and Ω_{log}=1.69 meV for Υ=0.25 meV), and hence λ_s must decrease to keep T_c constant.

The effect of the Coulomb pseudopotential is illustrated in Fig. 2, where the Ω_0 dependence of λ_s and Δ_d is shown for different values of μ_d^*, at fixed T_c=5 K. If μ_d^* increases from 0 to 0.2, Ω_0 increases up to about 2.5 meV, and λ_s up to about 3.1. We therefore conclude that magnetically mediated superconductivity in $NpPd_5Al_2$ requires spin fluctuations characterized by a dominating energy scale between 2 and 2.5 meV.

IV. ESTIMATION OF Ω_0 FROM NMR SPIN-LATTICE RELAXATION TIME

An experimental estimation of Ω_0 can be obtained from NMR measurements of $1/T_1$, the spin-lattice relaxation rate

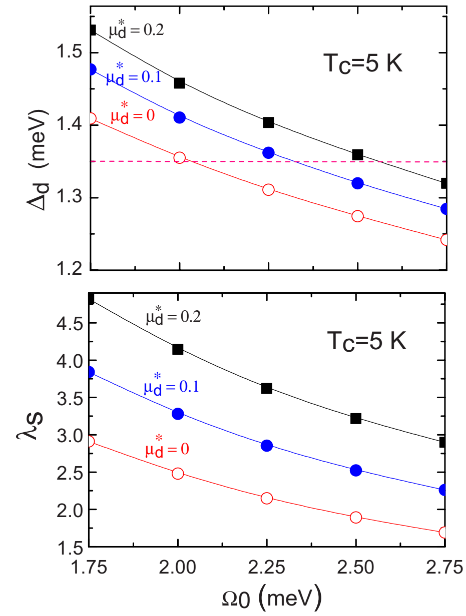

FIG. 2. (Color online) Gap values Δ_d (upper panel) and electron-boson coupling constant λ_s (lower panel) calculated at T=0.25 K assuming T_c=5 K and a Lorentzian-shaped boson spectral function with center at Ω_0 and full width at half maximum Υ=1 meV: (red, open circles) μ_d^*=0; (blue, closed circles) μ_d^*=0.1; (black squares) μ_d^*=0.2. The horizontal dashed line gives the experimental value of Δ_d.

at the Al site, in the normal state of $NpPd_5Al_2$.[20] Generally, $1/T_1$ is related to the dynamical magnetic susceptibility Im $\chi(\mathbf{q},\Omega)$,[27]

$$\frac{1}{T_1} = 2\gamma_N^2 T \sum_q A^2(q) \frac{\mathrm{Im}\,\chi(\mathbf{q},\omega_n)}{\omega_n}, \tag{6}$$

where γ_N, $A(q)$, and ω_n are the nuclear gyromagnetic ratio, the hyperfine coupling constant, and the NMR measurement frequency ($\sim$110 MHz in the present case), respectively. Since the hyperfine form factor $f^2(q)$=1 at the Al site of $NpPd_5Al_2$, and $A(q)\simeq A(0)f(q)$,[20]

$$\frac{1}{T_1} = 2\gamma_N^2 A^2(0) T \sum_q \frac{\mathrm{Im}\,\chi(\mathbf{q},\omega_n)}{\omega_n}. \tag{7}$$

The value of $A(0)$ has been determined by Chudo *et al.*[20] from the Knight shift versus static susceptibility plot. On the assumption that Im $\chi(\mathbf{q},\Omega)$ can be described in the Lorentzian form with the characteristic magnetic fluctuation energy Γ, one has

$$\frac{\mathrm{Im}\,\chi(\mathbf{q},\Omega)}{\Omega} \sim \frac{\chi(\mathbf{q})}{\Gamma_q}. \tag{8}$$

The q-averaged value of Γ can be determined from Eqs. (7) and (8) combined with the strong correlation approximation $2\pi\chi(q)\Gamma(q)\approx 1$,[28]

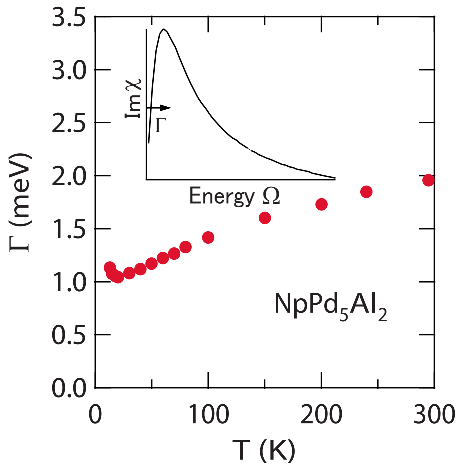

FIG. 3. (Color online) Temperature dependence of the characteristic magnetic fluctuation energy Γ in $NpPd_5Al_2$ estimated from the spin-lattice relaxation time NMR measurements at the Al site (Ref. 20). The inset shows the assumed Ω dependence of the dynamical susceptibility. The value of Γ corresponds to the energy of the maximum of the dynamical susceptibility.

$$\Gamma^2 = \frac{1}{\pi}\gamma_N^2 A^2(0) T_1 T. \tag{9}$$

Although it is q averaged, the above expression for Γ corresponds in the present case to that around the antiferromagnetic wave vector Q, for Im $\chi(\mathbf{q},\Omega)$ is enhanced around Q.[15]

Experiments have been performed on crystals aligned with the a or c crystallographic axis parallel to the external magnetic field and the isotropic part of Γ has been obtained as $\Gamma \equiv (2\Gamma_a + \Gamma_c)/3$. The results are shown in Fig. 3. The parameter Γ, whose value increases from about 1 to about 2 meV as the temperature increases up to 300 K, corresponds to the energy of the maximum of Im $\chi(\mathbf{q},\Omega)$, shown in the inset of Fig. 3, and can therefore be compared with the predicted value of Ω_0. The results obtained demonstrate that the characteristic magnetic fluctuation energy in $NpPd_5Al_2$ is of the correct order of magnitude to induce superconductivity below $T_c \simeq 5$ K.

V. OTHER OBSERVABLES

A. Upper critical field and penetration depth

The upper critical field H_{c2} can be calculated as a function of temperature by solving the linearized Eliashberg equations in presence of a magnetic field.[29,30] In the clean limit (negligible impurity scattering),

$$\omega_n Z_s(i\omega_n) = \omega_n + \pi T \sum_m \frac{1}{2\pi}\int_0^{2\pi} d\phi' \times \Lambda(i\omega_n - i\omega_m, \phi, \phi')\mathrm{sign}(\omega_m), \tag{10}$$

$$Z_s(i\omega_n)\Delta_d(i\omega_n,\phi) = \pi T \sum_m \frac{1}{2\pi}\int_0^{2\pi} d\phi' [\Lambda(i\omega_n - i\omega_m, \phi, \phi') - \mu_d^*(\omega_c,\phi,\phi')]\theta(\omega_c - |\omega_m|) \times \chi(i\omega_m) Z_s(i\omega_m)\Delta_d(i\omega_m,\phi'), \tag{11}$$

where

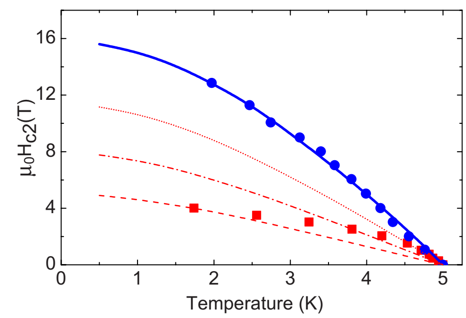

FIG. 4. (Color online) Temperature dependence of the upper critical field calculated for $T_c=5$ K, $\lambda_s=2.48$, $\mu_d^*=0$, $\Omega_0=2$ meV, and $\Upsilon=1$ meV. (Blue, solid line) Magnetic field **B** along the c crystallographic axis and Fermi velocity $v_F=0.569\times10^5$ m/s; (red, dotted-dashed line) **B** along the a crystallographic axis and $v_F=0.909\times10^5$ m/s; (red, dashed line) **B** along a and $v_F=1.170\times10^5$ m/s; (red, dotted line) **B** along a and $v_F=0.730\times10^5$ m/s. Experimental data are shown by blue circles (**B** along c) and red squares (**B** along a).

$$\chi(i\omega_m) = (2/\sqrt{\beta})\int_0^{+\infty} dq\, \exp(-q^2)\tan^{-1} \times \left[\frac{q\sqrt{\beta}}{|\omega_m Z_s(i\omega_m)| + i\mu_B H_{c2}\,\mathrm{sign}(\omega_m)}\right], \tag{12}$$

$\beta = \pi H_{c2} v_F^2/(2\Phi_0)$, v_F is the Fermi velocity, and Φ_0 is the unit of magnetic flux.

Figure 4 shows the comparison between experimental data[14] and $\mu_0 H_{c2}(T)$ curves calculated assuming $\lambda_s=2.48$ and $\Omega_0=2$ meV. For a field applied along the crystallographic c axis, the best fit is obtained for a Fermi velocity $v_F=0.569\times10^5$ m/s. Along the a crystallographic direction, the fit is less good and the experimental data are contained within the curves corresponding to $v_F=0.730\times10^5$ m/s and $v_F=1.17\times10^5$ m/s. The values of the Fermi velocity along different crystallographic directions are connected with cylindrical Fermi surfaces.[14]

The London penetration depth $\lambda(T)$ has been calculated following the procedure described in Ref. 31 and the results obtained are shown in Fig. 5. For this quantity, no experimental data are yet available.

B. Tunneling conductance and energy gap

The real-frequency-axis formulation of the Eliashberg theory allows one to calculate several physical quantities from the numerical solution of two coupled nonlinear singular integral equations involving a frequency- and temperature-dependent complex gap $\Delta(\omega,T)$ and a renormalization function $Z(\omega,T)$.[22] In the one-band, d-wave case one has[32,33]

$$\omega Z_s(\omega) = \omega + \Gamma_N \frac{N_Z(\omega)}{c^2 + N_Z^2(\omega)} + \int_{-\infty}^{+\infty} d\omega' \frac{1}{2\pi}\int_0^{2\pi} \times d\phi' \Lambda(\omega,\omega',\phi,\phi')\mathrm{Real}[N_Z(\omega',\phi')],$$

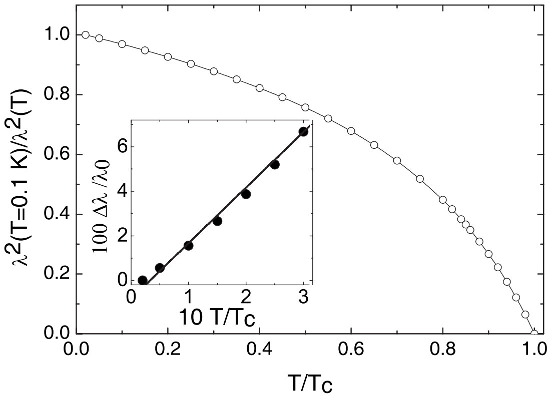

FIG. 5. Temperature dependence of the London penetration depth $\lambda(T)$ calculated for T_c=5 K, λ_s=2.48, μ_d^*=0, Ω_0=2 meV, and Υ=1 meV. The curve shows the values of $\lambda^2(T=0.1\ \text{K})/\lambda^2(T)$ as a function of the reduced temperature T/T_c. The low-temperature behavior is highlighted in the inset, showing $\Delta\lambda/\lambda_0=[\lambda(T)-\lambda(T=0.1\ \text{K})]/\lambda(T=0.1\ \text{K})$ versus T/T_c. The solid line is a linear fit of the results obtained from the numerical solution of the Eliashberg equations.

$$Z_s(\omega)\Delta_d(\omega,\phi)=\int_{-\infty}^{+\infty}d\omega'\frac{1}{2\pi}\int_0^{2\pi}d\phi'[\Lambda(\omega,\omega',\phi,\phi')-\mu_d^*(\omega_c,\phi,\phi')\theta(\omega_c-|\omega'|)]\times\mathrm{Real}[N_\Delta(\omega',\phi')] \quad (13)$$

with

$$\Lambda(\omega,\omega',\phi,\phi')=\frac{1}{2}\int_0^{+\infty}d\Omega\alpha^2F(\Omega,\phi,\phi')\times\left[\frac{\tanh\left(\frac{\omega'}{2T}\right)+\coth\left(\frac{\Omega}{2T}\right)}{\omega'+\Omega-\omega-i\delta}-\frac{\tanh\left(\frac{\omega'}{2T}\right)-\coth\left(\frac{\Omega}{2T}\right)}{\omega'-\Omega-\omega-i\delta}\right], \quad (14)$$

the superconductive density of states being equal to

$$(1/2\pi)\mathrm{Real}[\textstyle\int_0^{2\pi}d\phi' N_Z(\omega,\phi')],$$

$$N_Z(\omega,\phi)=\omega/\sqrt{\omega^2-\Delta^2(\omega,\phi)},$$

and

$$N_\Delta(\omega,\phi)=\Delta(\omega,\phi)/\sqrt{\omega^2-\Delta^2(\omega,\phi)}.$$

The numerical solutions of the above equations, obtained for Ω_0=2 meV, Υ=1 meV, and μ_d^*=0, have been used to calculate the temperature dependence of the energy gap, and the energy dependence of the tunneling differential conductance at different temperatures. The obtained curves are shown in Fig. 6. The differential conductance can be obtained from the current-voltage characteristic of a metal-insulator-superconductor tunneling junction, and at zero temperature it coincides with the normalized quasiparticle density of states. Point-contact spectroscopy measurements to determine these quantities are planned at ITU.

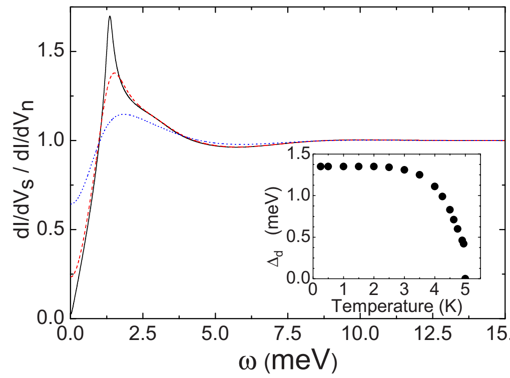

FIG. 6. (Color online) Energy dependence of the tunneling differential conductance calculated in the superconducting phase of $NpPd_5Al_2$ assuming T_c=5 K, λ_s=2.48, μ_d^*=0, Ω_0=2 meV, and Υ=1 meV. Black solid line: T=0.25 K; red dashed line: T=2 K; blue dotted line: T=4 K. The inset shows the temperature dependence of the energy gap calculated for the same set of parameters.

C. Local spin susceptibility and spin-lattice relaxation rate

Finally, we have calculated the temperature dependence of the local spin susceptibility χ and of the nuclear-spin-lattice relaxation rate T_1^{-1} in the superconducting phase of

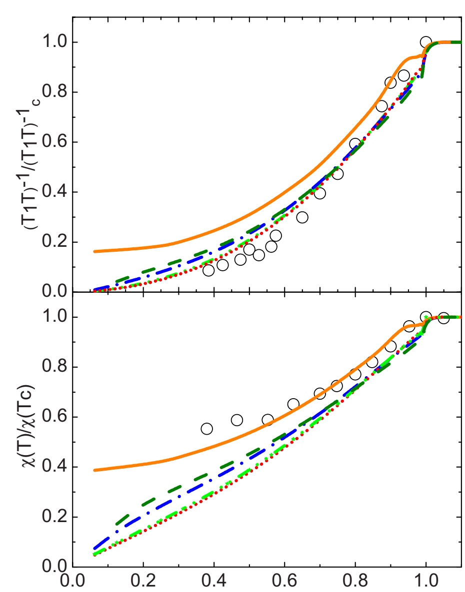

FIG. 7. (Color online) Temperature dependence of (upper panel) the normalized nuclear spin-relaxation rate, $(T_1T)^{-1}/(T_1T)_c^{-1}$, and (lower panel) the normalized local spin susceptibility, $\chi(T)/\chi(T_c)$, calculated in the superconducting phase of $NpPd_5Al_2$, assuming λ_s=2.48, μ_d^*=0, Ω_0=2 meV, Υ=1 meV, and several different sets of values for the c and Γ parameters: (solid orange line) c=0 and Γ=0.391 meV; (olive dash line) c=0.5 and Γ=0.4885 meV; (blue dashed-dotted line) c=1 and Γ=0.782 meV; (red dotted line) $c=\infty$ and Γ/c=0.391 meV; (green dashed-dotted-dotted line) c=3 and Γ=3.91 meV. Experimental data are shown by open circles.

$NpPd_5Al_2$, and compared the results with the experimental data obtained by Chudo *et al.*[11] from ^{27}Al NMR measurements. The data were collected in presence of a magnetic field, reducing the critical temperature to 4 K. This reduction has been simulated in the calculations by introducing an impurity-scattering parameter Γ (Ref. 34) leading to the correct value of T_c. We assumed $\lambda_s=2.48$, $\mu_d^*=0$, $\Omega_0=2$ meV, $\Upsilon=1$ meV, and different sets of values for the c and Γ_N parameters, going from the unitary limit ($c=0$ and $\Gamma_N=0.391$ meV) to the Born limit ($c=\infty$ and $\Gamma_N/c=0.391$ meV).[8] The calculated and measured curves, normalized at the values assumed at $T=T_c$, are shown in Fig. 7. For the local spin susceptibility, a good agreement is obtained in the unitary limit. On the other hand, the experimental behavior of the spin-lattice relaxation rate is better described in the Born limit. Despite this discrepancy, the overall qualitative agreement is as good as can be expected, considering the approximations we used in our simple *d*-wave model.

VI. CONCLUSIONS

The Eliashberg theory of superconductivity has been used to estimate the energy scale Ω_0 of the electron-boson spectral function in the heavy-fermion, *d*-wave superconductor $NpPd_5Al_2$. Assuming a spectral function shape typical for antiferromagnetic spin fluctuations and imposing constraints provided by the experimental values for the critical temperature and the low-temperature energy gap, we predict values of Ω_0 of about 2–2.5 meV, slightly dependent from the strength of the Coulomb pseudopotential. Although the calculations presented here are independent from the particular nature of the Cooper-pair mediating bosons, the observation by NMR experiments of spin fluctuations with a maximum spectral weight at energies close to the predicted value of Ω_0 provide further support to the hypothesis of magnetically mediated superconductivity in $NpPd_5Al_2$. Inelastic neutron-scattering experiments would be interesting to confirm the proposed scenario.

Calculations provide values for the electron-boson coupling constant λ_s of about 2.5, confirming that $NpPd_5Al_2$ is a strong-coupling superconductor. Finally, we used the solutions of the Eliashberg equations to calculate the temperature dependence of several physical quantities, such as the upper critical field, the London penetration depth, the local spin susceptibility, the nuclear-spin-lattice relaxation rate, and the energy gap, as well as the energy dependence of the tunneling differential conductance at various temperatures. The calculated curves compare favorably with available experimental data and provide predictions for future experimental work.

ACKNOWLEDGMENTS

This work is partially supported by the Reimei research program of JAEA. S.K. is supported by a Grant-in-Aid for Scientific Research on Innovative Areas "Heavy Electrons" of The Ministry of Education, Culture, Sports, Science, and Technology, Japan.

[1] P. Santini, S. Carretta, G. Amoretti, R. Caciuffo, N. Magnani, and G. H. Lander, Rev. Mod. Phys. **81**, 807 (2009).
[2] K. T. Moore and G. van der Laan, Rev. Mod. Phys. **81**, 235 (2009).
[3] C. Pfleiderer, Rev. Mod. Phys. **81**, 1551 (2009).
[4] J. L. Sarrao, L. A. Morales, J. D. Thompson, B. L. Scott, G. R. Stewart, F. Wastin, J. Rebizant, P. Boulet, E. Colineau, and G. H. Lander, Nature (London) **420**, 297 (2002).
[5] D. Aoki *et al.*, J. Phys. Soc. Jpn. **76**, 063701 (2007).
[6] F. Jutier, G. A. Ummarino, J.-C. Griveau, F. Wastin, E. Colineau, J. Rebizant, N. Magnani, and R. Caciuffo, Phys. Rev. B **77**, 024521 (2008).
[7] A. Hiess, A. Stunault, E. Colineau, J. Rebizant, F. Wastin, R. Caciuffo, and G. H. Lander, Phys. Rev. Lett. **100**, 076403 (2008).
[8] G. Ummarino, N. Magnani, J.-C. Griveau, J. Rebizant, and R. Caciuffo, J. Nucl. Mater. **385**, 4 (2009).
[9] Y. Haga *et al.*, J. Alloys Compd. **464**, 47 (2008).
[10] J.-C. Griveau, K. Gofryk, and J. Rebizant, Phys. Rev. B **77**, 212502 (2008).
[11] H. Chudo *et al.*, J. Phys. Soc. Jpn. **77**, 083702 (2008).
[12] K. Gofryk, J.-C. Griveau, E. Colineau, J. P. Sanchez, J. Rebizant, and R. Caciuffo, Phys. Rev. B **79**, 134525 (2009).
[13] F. Honda *et al.*, J. Phys. Soc. Jpn. **77** Suppl. A, 043701 (2008).
[14] H. Yamagami, D. Aoki, Y. Haga, and Y. Ōnuki, J. Phys. Soc. Jpn. **76**, 083708 (2007).
[15] K. Tanaka and K. Hanzawa, J. Phys. Soc. Jpn. **78**, 044705 (2009).
[16] P. Monthoux and G. G. Lonzarich, Phys. Rev. B **63**, 054529 (2001).
[17] G. M. Eliashberg, Sov. Phys. JETP **11**, 696 (1960).
[18] J. P. Carbotte, Rev. Mod. Phys. **62**, 1027 (1990).
[19] F. Marsiglio, J. Low Temp. Phys. **87**, 659 (1992).
[20] H. Chudo, H. Sakai, Y. Tokunaga, S. Kambe, D. Aoki, Y. Homma, Y. Haga, T. D. Matsuda, Y. Ōnuki, and H. Yasuoka, J. Phys. Soc. Jpn. **79**, 053704 (2010).
[21] C. T. Rieck, D. Fay, and L. Tewordt, Phys. Rev. B **41**, 7289 (1990).
[22] J. P. Carbotte and C. Jiang, Phys. Rev. B **49**, 6126 (1994).
[23] S. K. Bose, O. V. Dolgov, J. Kortus, O. Jepsen, and O. K. Andersen, Phys. Rev. B **67**, 214518 (2003).
[24] H. Vidberg and J. Serene, J. Low Temp. Phys. **29**, 179 (1977).
[25] C. Leavens and D. Ritchie, Solid State Commun. **53**, 137 (1985).
[26] G. A. Ummarino and R. S. Gonnelli, Physica C **328**, 189 (1999).
[27] T. Moriya, *Spin Fluctuations in Itinerant Electron Magnetism* (Springer-Verlag, Berlin, 1985).
[28] H. Shiba, Prog. Theor. Phys. **54**, 967 (1975).
[29] G. A. Ummarino, Physica C **423**, 96 (2005).
[30] M. Schossmann and E. Schachinger, Phys. Rev. B **33**, 6123

(1986).

[31] A. A. Golubov, A. Brinkman, O. V. Dolgov, J. Kortus, and O. Jepsen, Phys. Rev. B **66**, 054524 (2002).

[32] G. A. Ummarino, D. Daghero, and R. S. Gonnelli, Physica C **377**, 292 (2002).

[33] P. B. Allen and B. Mitrovich, *Solid State Physics* (Academic, New York, 1982), Vol. 37.

[34] J. M. Daams, H. G. Zarate, and J. P. Carbotte, Phys. Rev. B **30**, 2577 (1984).